JOURNAL OF SPACECRAFT AND ROCKETS
Vol. 29, No. 6, November–December 1992

Buffet Loads Prediction for a Launch Vehicle and Comparison to Flight Data

Mohamed M. Ragab*
General Dynamics Space Systems Division, San Diego, California 92186

A comparison of preflight predictions of the Atlas I launch vehicle dynamic response to the values measured in flight indicates that the current prediction methods are very conservative. An overview of the wind-tunnel tests performed during the development of the large payload fairing for Atlas I is presented. The results of buffet analysis with forcing functions based on the wind-tunnel-measured fluctuating pressures are compared to previous configuration flight data. Buffet forcing functions based on flight data are also developed. The exceedence of the flight data at about 10 Hz relative to buffet analysis results is attributed to gust excitation. The deviation of the transonics flight data-derived buffet forcing functions above 20 Hz relative to the wind-tunnel- and flight-measured external oscillatory buffet pressures can be attributed to the fact that, in the analysis, the acoustic excitation was not being applied directly on the spacecraft. Some areas of future research are proposed to improve the accuracy of prediction of the atmospheric environment and space vehicle response, and, therefore, provide important opportunities for improving the performance and increasing the reliability of space vehicles.

Nomenclature

A = payload fairing cross-sectional (frontal) area, in.^{2}
C_σ = bending moment coefficient, $= \sigma/QAD$
D = maximum payload fairing diameter, in.
M = Mach number
m = bending moment, in.-lb
Q = dynamic pressure, lb/in.^{2}
α = angle of attack, deg
β = angle of side slip, deg
σ = root-mean-square bending moment, in.-lb

Subscripts
B = buffet
D = dispersions
G = gust
LC = limit cycle
P = persistence
WO = wind only

Sub-subscripts
m = mean
r = random

Introduction

TO a large extent, space vehicle design is governed by the severe environments to which the vehicles are subjected during atmospheric ascent. The success of such designs depends on understanding and accurately predicting those environments and the vehicle's response.

In the late 1950s, a series of launch vehicle failures occurred during the transonic portion of their atmospheric ascent. Buffet had not been considered in the design of these early vehicles. The intensive research on launch vehicle buffet in the 1960s made successful designs possible. A review of the progress made in the early years can be found in Ref. 1. Reference 2 is a general survey of the field of space vehicle structural vibration, which is induced by acoustic and aerodynamic noise and certain mechanical excitations. Publications describing work done on individual launch vehicle configurations, such as Refs. 3–5, can also be found, although the number of recent publications on the subject is very limited. Reliable methods for analytical prediction of vehicle stability and buffet response by computational fluid dynamics techniques are not yet available, although significant advances have been reported recently, such as in Ref. 6.

Today, the state of the art of predicting the atmospheric environment of space vehicles is such that a large proportion of the predicted loads never actually occur during flight. However, it is necessary to cover all of the uncertainties in order to ensure a very high probability of mission success. On the other hand, the state of the art of space vehicle design, given a specific set of design loads, is such that relatively small improvements in system performance can be obtained without undesirably large expenses in cost and system complexity. Research work leading to improved accuracy of prediction of the atmospheric environment and space vehicle response will therefore provide important opportunities for improving the performance and increasing the reliability of space vehicles.

In this paper, a brief description of the different types of environments encountered by space vehicles during atmospheric ascent will be presented and the relative importance of the different flight wind load components will be discussed. The degree of conservatism in the prediction of flight loads will be illustrated by a comparison of preflight prediction of Atlas I engine gimbal angle and bending moment time histories to the values measured in flight.

The prediction of buffet loads for the Atlas I launch vehicle will then be presented. The use of both wind-tunnel test data and flight data will be discussed, and the difficulties and limitations associated with each of these data sources will be shown. Explanations will be given for an exceedence of the flight data relative to buffet analysis results, and the deviation of the flight data-based buffet forcing functions relative to wind-tunnel and flight measurements of external oscillatory buffet pressures.

Space Vehicle Environment and Flight Loads

Natural and Induced Environment

The space vehicle environment can be divided into two major types, the natural environment and the induced envi-

Presented as Paper 92-0716 at the AIAA 30th Aerospace Sciences Meeting and Exhibit, Reno, NV, Jan. 6–9, 1992; received Jan. 16, 1992; revision received July 30, 1992; accepted for publication Aug. 4, 1992.

*Engineering Specialist, Launch Vehicle Engineering. Senior Member AIAA.

ronment. The natural environment is that which exists irrespective of whether the vehicle is present or not. Examples include flight winds and ambient atmospheric temperature and pressure. The induced environment is caused by the presence of the space vehicle or its operation. Examples include vibration and acoustics due to rocket engine operation, shock during staging, and buffet. A major difference concerning the characterization of those two types of environments is that the natural environment is common to all vehicles and can therefore be studied independently, while the induced environment is specific to each vehicle, must be the subject of specific studies, and is a function of the vehicle's design parameters. Studies of the natural environment should, however, draw upon the flight experience gained during the testing and operation of different space vehicles.

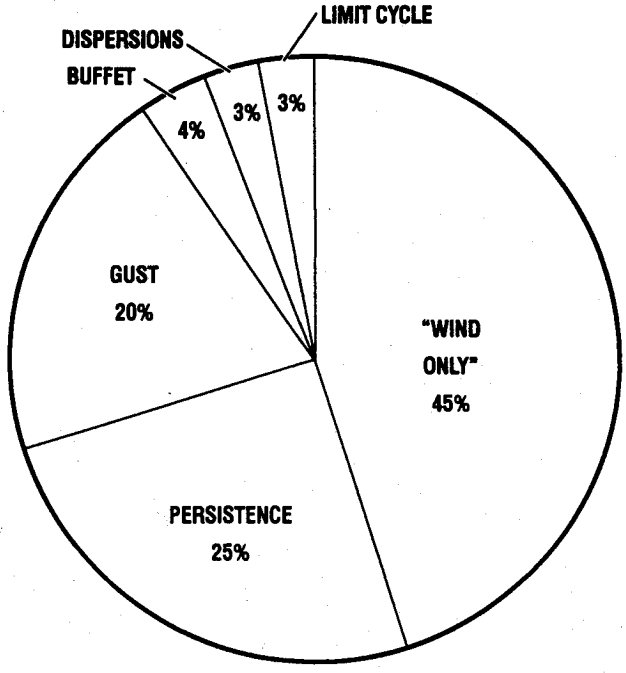

Fig. 1 Relative importance of flight wind load components.

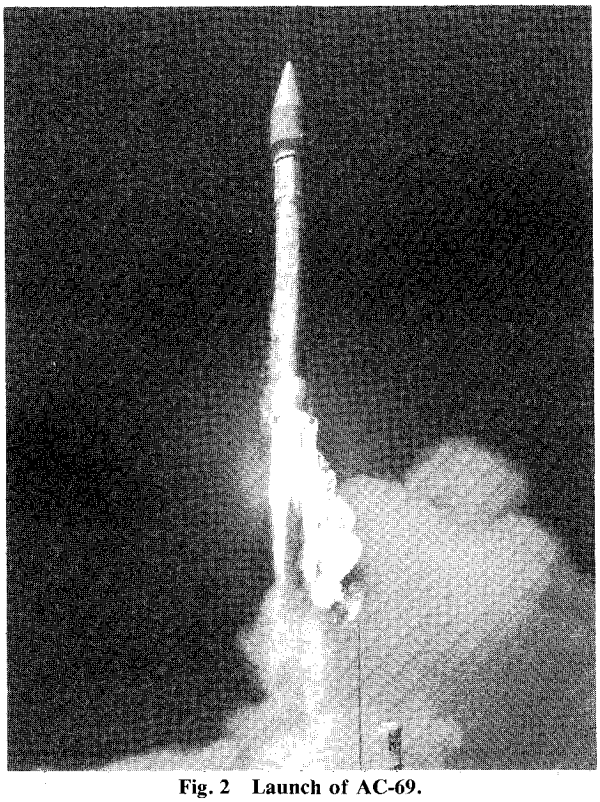

Fig. 2 Launch of AC-69.

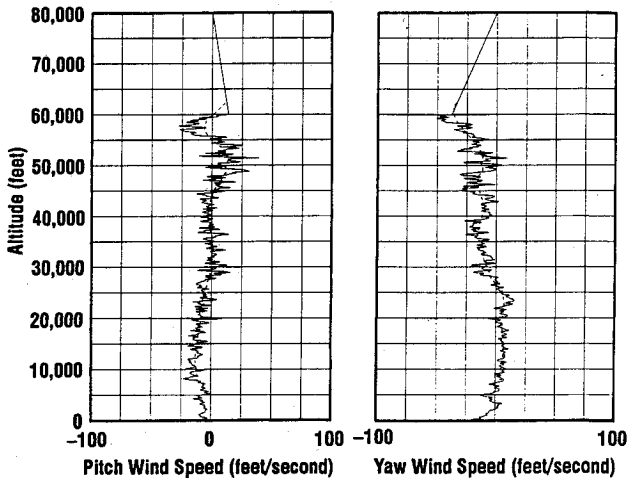

Fig. 3 AC-69 L-25 Rawinsonde balloon measurement.

Load Components During Atmospheric Flight

Flight wind load components can be divided into two categories based on the time at which they are calculated. The so-called "wind only" loads are calculated based on the wind profile measured as close as practical before the flight, while the precalculated loads are, as their name implies, calculated long before launch day operations. Wind-only loads for Atlas/Centaur vehicles are minimized by using pitch and yaw steering designed for zero angles of attack and sideslip relative to a filtered wind profile during the high loading portion of the flight. Precalculated loads for Atlas/Centaur are due to persistence (which accounts for the change in the wind profile between the wind measurement and the actual flight), gust, buffet, dispersions of the different analysis parameters, and control system limit cycling.

To calculate the bending moment at a given flight time and vehicle station, the following loads combination equation is used.

$$m = m_{WO} + m_{P_m} + m_{G_m} + m_{LC_m} + (m_{P_r}^2 + m_{G_r}^2 + m_B^2 + \sum m_D^2 + m_{LC_r}^2)^{1/2} \quad (1)$$

The components that are root-sum-squared are assumed to be uncorrelated. It has been shown recently that limit cycling need not be considered during the high loads portion of the flight. Figure 1 shows a sample relative importance of those loading components, limit cycle included, as was the case during Atlas I development. The exact percentage of contribution of each depends on the flight condition and station considered. However, this chart can still be used to assess the importance of the potential benefit to be gained from future research work in each of the load components, as the relative importance does not significantly change.

Comparison to Flight Data

First Atlas I Flight

The first commercial Atlas/Centaur, Atlas I vehicle AC-69, was successfully launched from Cape Canaveral on July 25, 1990 (Fig. 2) carrying the USAF/NASA Combined Release and Radiation Effects Satellite (CRRES). Figure 3 shows the launch minus 25 min (L-25) release time Rawinsonde balloon wind measurement, which is the best available data for the flight winds encountered during the AC-69 flight since it takes about 55 min for the Rawinsonde to reach 60,000 ft altitude. Notice the more severe wind shears that the vehicle would encounter in the 45,000–60,000 ft altitude range as the dynamic pressure has already started to drop with altitude.

Engine Gimbal Angle Time History

A comparison of preflight prediction of Atlas engine gimbal angle time history to the values measured in flight is shown in Fig. 4. The L-150 Jimsphere wind measurement calculation, which includes allowance for precalculated loads, is the one used for the flight pitch and yaw steering design and the primary launch go/no-go decision for flight winds. It predicted a maximum engine gimbal angle about twice what was actually measured in flight. The fact that the prediction was very conservative is quite typical of the Atlas/Centaur flight experience.[7] The much closer proximity to flight data of the maximum engine angle prediction of the L-25 wind only is also in line with the previous flight experience.

Bending Moment Correlation with Engine Gimbal Angle

The booster engine gimbal angle correlates very well with the low-frequency portion of the flight bending moments. This can be seen in the two AC-69 flight time histories displayed in Fig. 5 as well as the cross plotting of the time histories shown in Fig. 6. The bending moments were measured by strain gauges mounted in the maximum bending moment location in the Atlas LO_2 tank. The yaw direction was chosen here because the maximum engine gimbal angle that occurred shortly before 95 s was mostly in yaw. Also plotted in Fig. 6 is a straight line through the origin with a slope of 2.19×10^6 in.-lb/deg, which is the value obtained from the static aeroelastic analysis at $M = 1.65$ and $\beta = 1$ deg performed for Atlas I development. Although the slope is a function of the flight condition, Fig. 6 shows that slope practically at the center of the flight response. That indicates very good correlation. The maximum bending moment deviation from that static aeroelastic analysis prediction due to dynamic responses is about 28% of the maximum bending moment value for that flight.

Evaluation of Space Vehicle Buffet Loads

Although the buffet loading component is not one of the three major load components for the Atlas/Centaur, buffet clearly illustrates the general problem of atmospheric environment characterization and prediction of space vehicle response because it is one of the most difficult, if not the most difficult to predict. Buffet is an induced environment and due to its nature, statistical methods are used for analysis, and comparisons with flight data are used to complement the wind-tunnel test data. This is necessary because accurate analytical predictions of buffet loads cannot be achieved unless very detailed measurements of pressure are used, including complete cross-correlation between all points of pressure measurement.

Buffet Loads Based on Wind-Tunnel Test Data

Wind-Tunnel Tests

During the development of the large payload fairing (LPF) and medium payload fairing for Atlas/Centaur, two series of wind-tunnel tests were performed. The first series used a 1/23rd-scale rigid model in the NASA Lewis Research Center transonic wind tunnel. Seventy-five Kulite oscillatory pressure transducers were included in the instrumentation. The second series of tests used a 1/10th-scale rigid forebody model with elastic hinges at the forward nodes aeroelastically scaled to simulate either the first or the second bending modes of the full-scale vehicle. The model was tested in the NASA Langley Research Center Transonic Dynamics Tunnel. The primary objective of the first series of tests was to collect pressure data for vehicle loads evaluation while the second series was primarily concerned with buffet response and dynamic stability. Figure 7 shows a typical pressure power spectral density (PSD) vs model frequency from the 1/23-scale wind-tunnel test. The

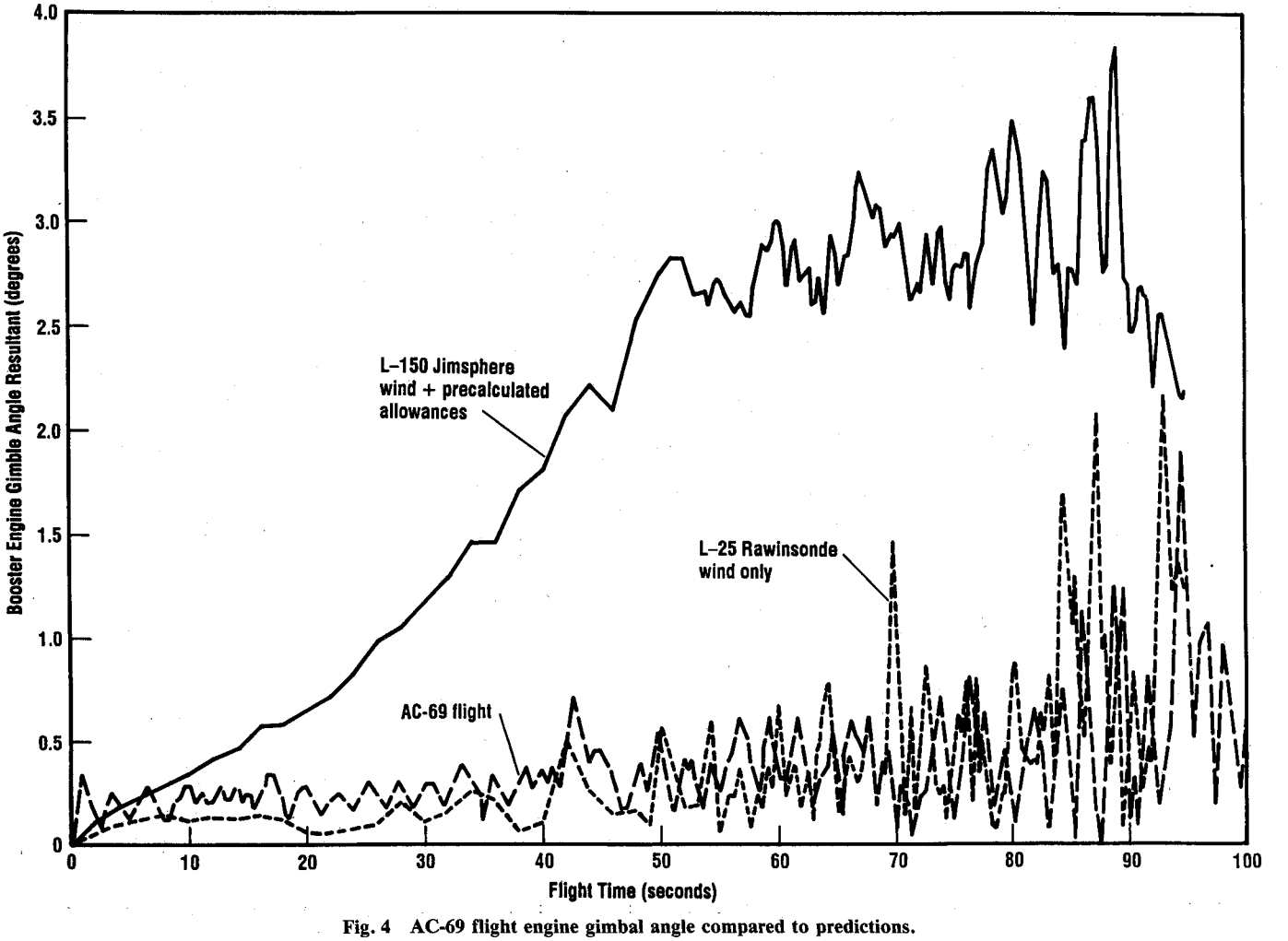

Fig. 4 AC-69 flight engine gimbal angle compared to predictions.

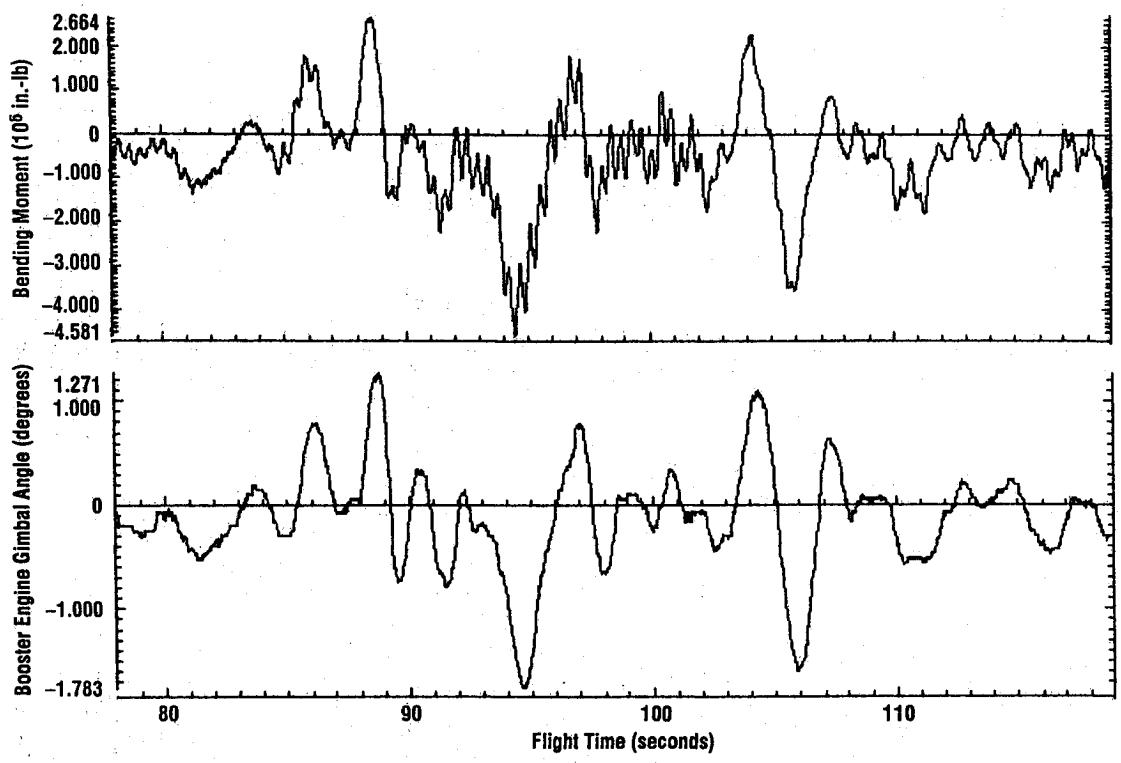

Fig. 5 AC-69 yaw plane flight response.

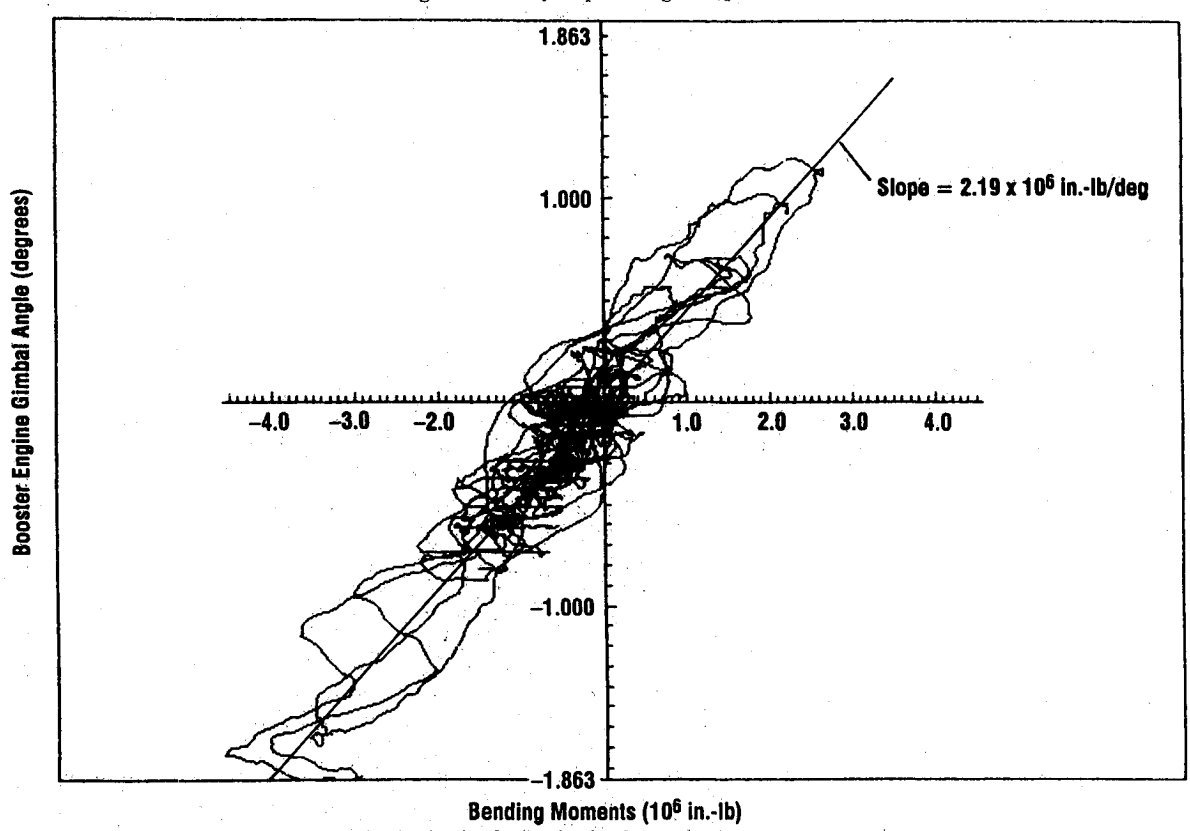

Fig. 6 AC-69 yaw plane flight-measured bending moment vs engine gimbal angle.

model frequency of 1200 Hz corresponds to 52.2-Hz full scale. The data shown is for the bottom of the LPF cylindrical section for Mach 0.85 and zero angles of attack and sideslip. Notice the general trend of fluctuating pressure decrease with frequency with the exception of the peaks around 800-Hz model frequency, which are data anomalies due to wind-tunnel compressor noise.[8]

Buffet Forcing Function Development

Buffet forcing functions were derived based on the wind-tunnel test data with the conservative assumptions that buffet pressures act on one side of the vehicle only and with unit correlation. The forces were scaled to an Atlas G 10-ft-diam fairing for comparison to available flight data. The forces were applied at points A and B as shown in Fig. 8 as suggested by the wind-tunnel pressure distribution. Figures 9 and 10 show the Atlas G transonics and maximum dynamic pressure (max Q) forcing functions. The general trend of fluctuating pressure decrease with frequency is the same for both cases.

Data from Previous Configuration Flights

The most consistent set of flight data available was from the

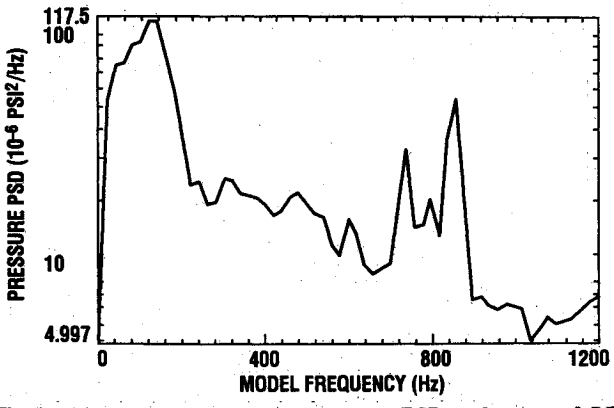

Fig. 7 1/23rd-scale wind tunnel pressure PSD at bottom of LPF cylindrical section ($M = 0.85$, $\alpha = \beta = 0$).

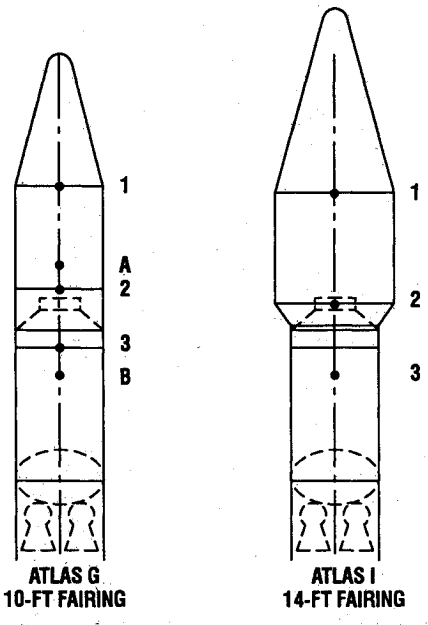

Fig. 8 Input force locations on Atlas G and Atlas I models.

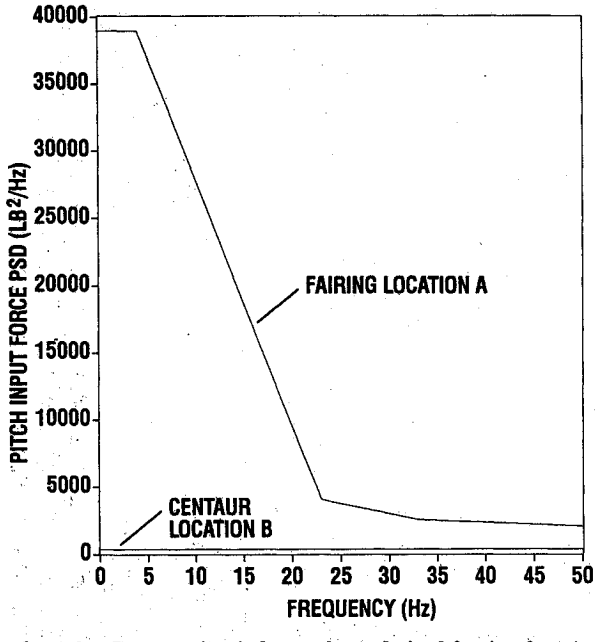

Fig. 9 Atlas G transonic wind-tunnel test derived forcing functions.

Atlas SLV-3D/Intelsat V and Atlas G/Intelsat VA flights. The flight data of both configurations are very similar and are treated here as one set of data. The available data consisted of launch vehicle/spacecraft interface accelerations in pitch and yaw for a total of 10 flights and spacecraft forward deck accelerations for 7 flights in pitch and for 5 flights in yaw. PSDs were generated for 2-s intervals using a Hanning window for transonics through max Q and 0–50 Hz for the interface acceleration data. An envelope of all PSDs was used. Peak accelerations for interface accelerometer transonics and max Q and spacecraft accelerometer transonics data were also obtained for 99% probability and 90% confidence statistics.

Correlation to the Flight Data

The multimode random response analysis procedure of Ref. 9 was used for calculating response PSDs and root-mean-square (rms) values. Figure 11 shows a comparison of the interface response to transonic wind-tunnel test-derived forcing functions relative to flight data. That comparison indicates a need for a knock-down factor on the order of one-fifth in the low-frequency range compared to analytical responses determined by applying the fluctuating pressure on one side of the vehicle only and a need for an increase in the high-frequency range. That assessment is conservative, however, due to the difficulty of separating the portions of flight data due to different loading sources that occur simultaneously (e.g., gust, buffet, and acoustics) including any local shell vibration at the accelerometer location. Notice that the flight data exceeds the analysis results at about 10 Hz. That exceedence will be even larger with the application of a knock-down factor in the low-frequency range. Therefore, the flight response at about 10 Hz is not buffet-related and is attributed to gust excitation.

Buffet Loads Based on Flight Data

Development of Forcing Functions

Forcing functions were also developed to envelope the flight data. The forces were applied at locations 1, 2, and 3 of Fig. 8, where they were found to be most effective. Pitch input force PSDs are shown for Atlas G for the transonic and max Q cases in Figs. 12 and 13. A comparison of the responses to the transonic forcing functions vs flight data is shown in Fig. 14. As before, the exceedence of the flight data relative to analysis results at about 10 Hz was attributed to gust excitation. The frequency mismatch at the higher frequencies is believed to be related to the forcing function magnitude, which will be addressed in the next two paragraphs.

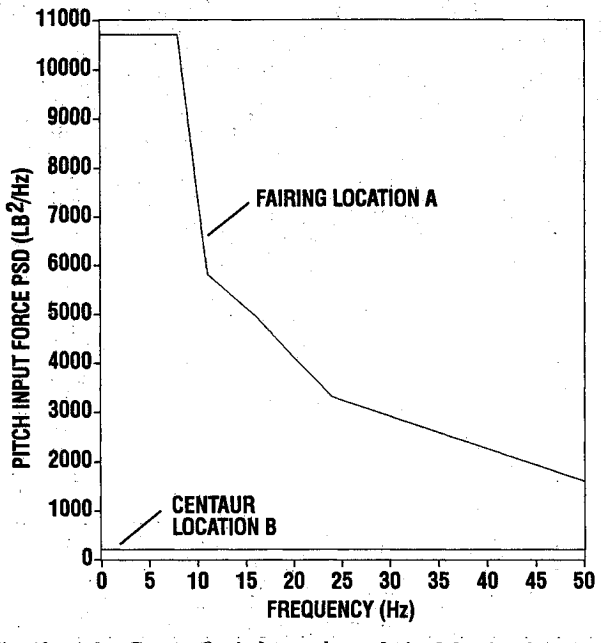

Fig. 10 Atlas G max-Q wind-tunnel test derived forcing functions.

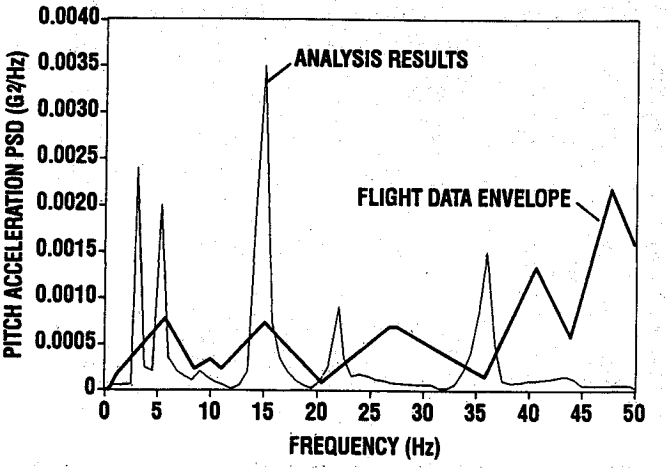

Fig. 11 Atlas G/Intelsat VA interface response to transonic wind-tunnel test-derived forcing functions compared to flight data.

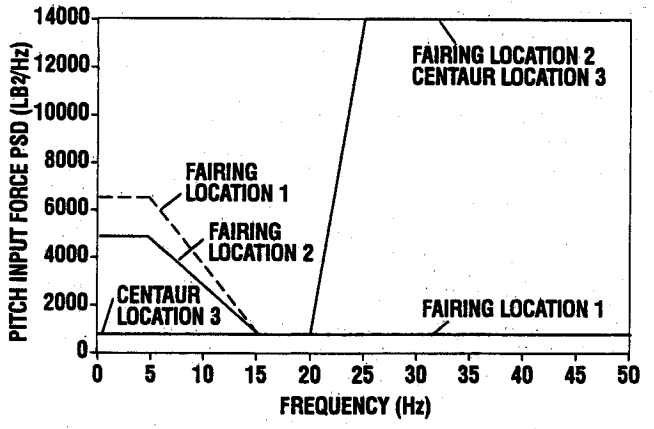

Fig. 12 Atlas G transonic flight data-derived forcing functions.

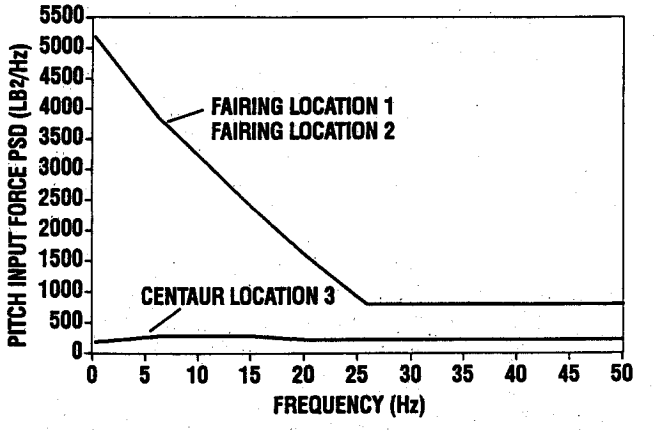

Fig. 13 Atlas G max-Q flight data-derived forcing functions.

Limitations of Flight Data-Based Forcing Functions

Although the variation of the magnitude of the flight data-based forcing functions as function of frequency for the maximum dynamic pressure case is similar to the wind-tunnel measured data, that was not the case for the transonics time of flight. Instead of decaying to low values at 20–25 Hz and above, the magnitude of the forcing function increased again above 20–25 Hz to values higher than those in the low-frequency range for the transonic time of flight. Figure 15 shows the AC-69 flight boattail fluctuating pressure PSD for the 60–61 s time of flight (about Mach 0.85). Flight data show decreasing fluctuating pressures as a function of frequency for that transonic time of flight. The AC-69 transonic flight data-derived forcing function shown in Fig. 16 (refer to Fig. 8 for locations) also follows the same trend. The deviation of higher buffet forces above 20 Hz is therefore incompatible with the spectra derived from wind-tunnel and flight measurements of external oscillatory buffet pressures, and applying these forces externally results in spacecraft forward deck acceleration responses that are about 12 times higher than those actually occurring in flight. It is also interesting to compare the AC-69 first bending mode coefficients to the 1/10th-scale wind-tunnel test data.[5] As shown in Fig. 17, the flight bending moment coefficient follows the wind tunnel 1σ data rather closely. The departure of the wind-tunnel data beyond Mach 1.0 is possibly due to wind-tunnel facility mechanical vibration.

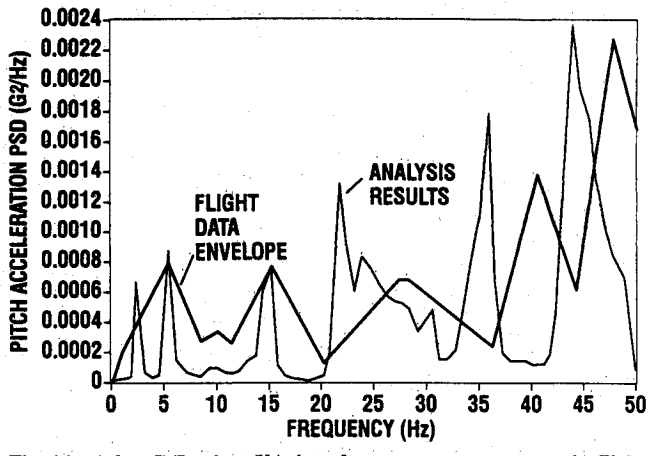

Fig. 14 Atlas G/Intelsat VA interface response to transonic flight data-derived forcing functions compared to flight data.

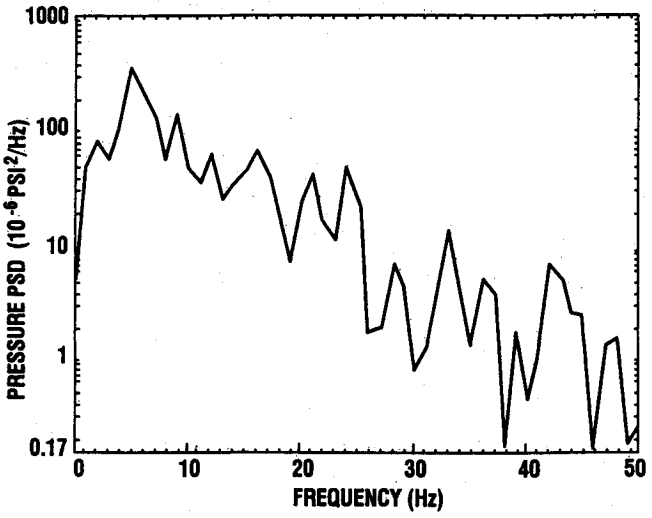

Fig. 15 AC-69 flight boattail pressure PSD for 60–61 s time of flight.

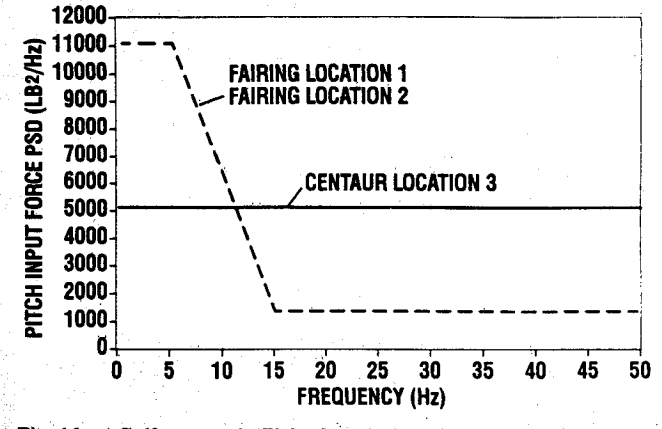

Fig. 16 AC-69 transonic flight data-derived forcing functions.

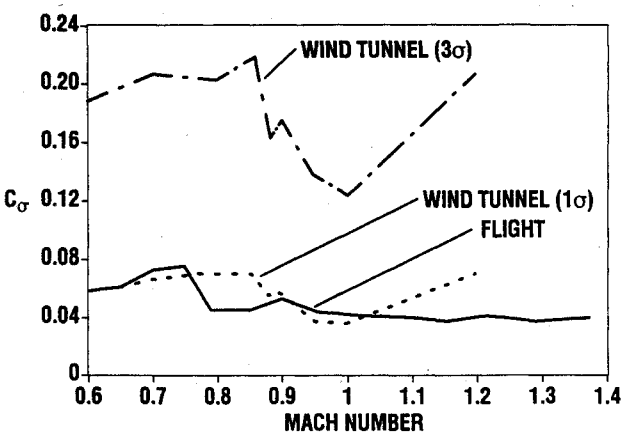

Fig. 17 AC-69 flight first bending mode bending moment coefficient compared to wind-tunnel data.

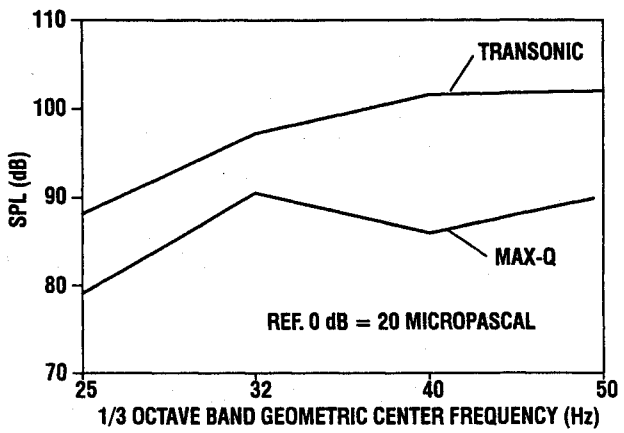

Fig. 18 AC-69 flight maximum measured internal sound pressure level.

Acoustic Environment Contribution

The flight data-derived forcing functions assumed that all of the response measured in flight was due to buffet. To explain the deviation of buffet forces above 20 Hz, other loading sources were considered. The acoustic environment inside the payload fairing follows the same trend as a function of frequency as the flight-derived buffet forces and is about 10 dB higher at transonics relative to maximum dynamic pressure, as shown in Fig. 18. Moreover, acoustic loads can produce high-level responses, as evidenced by the response levels at liftoff or during acoustic testing. Therefore, the need to increase the forcing function in the 20–50 Hz region could be attributed to the fact that, in the analysis, the acoustic excitation was not being applied directly on the spacecraft.

Conclusions

Comparison of Atlas I flight data to preflight predictions showed that current methods of prediction are very conservative. Careful examination of wind-tunnel test data and previous flight data was required to evaluate the contribution of buffet for space vehicle loads analysis. The exceedence of the flight data relative to buffet analysis results at about 10 Hz was attributed to gust excitation. The deviation of the transonics flight data-derived buffet forcing functions above 20 Hz, relative to the wind tunnel and flight-measured external oscillatory buffet pressures, could be attributed to the fact that, in the analysis, the acoustic excitation was not being applied directly on the spacecraft. Important opportunities exist for improving the performance and increasing the reliability of space vehicles by more accurately predicting the atmospheric environment and space vehicle response. Additional flight data and new methods are therefore needed. Some areas of future research suggested include additional methods for determining the different load contributions to flight-measured responses, and methods to calculate spacecraft response to acoustic loads and to evaluate the gust portion of the load calculated based on the day of launch wind measurement, in addition to reducing the time needed to get the wind profile measurement.

Acknowledgments

This work was partially supported by U.S. Air Force Space Systems Division Contract F04701-88-C-0042. K.W. McGuinness of General Dynamics performed the buffet analysis using the Ref. 3 code as suggested by A. M. Kabe of The Aerospace Corporation.

References

[1]Rainey, A. G., "Progress on the Launch Vehicle Buffeting Problem," *Journal of Spacecraft and Rockets,* Vol. 2, No. 3, 1965, pp. 289–299.

[2]Himelbau, H., Fuller, C. M., and Scharton, T. D., "Assessment of Space Vehicle Aeroacoustic-Vibration Prediction, Design, and Testing," NASA CR-1596, July 1970.

[3]Bombardier, G. D., "Final Post-Test Report on Seven Percent Transonic Buffet Model for Various Titan III Configurations," Martin Co., SSD-CR-66-563, Denver, CO, Jan. 1967.

[4]Coe, C. F., "Buffet Loads on Shuttle Thermal-Protection System Tiles," *The Shock and Vibration Bulletin,* No. 52, Pt. 2, May 1982, pp. 147–153.

[5]Cole, S. R., and Henning, T. L., "Buffet Response of a Hammerhead Launch Vehicle Wind Tunnel Model," *Journal of Spacecraft and Rockets,* Vol. 29, No. 3, 1992, pp. 379–385; see also AIAA Paper 91-1050.

[6]de Azevedo, J. L. F., "Transonic Aeroelastic Analysis of Launch Vehicle Configurations," NASA CR-4186, Oct. 1988.

[7]Martin, R.E., "Atlas I Analyses and Environments Validation," International Astronautical Federation, Paper 91-170, Oct. 1991.

[8]Karabinus, R. J., and Sanders, B. W., "Measurements of Fluctuating Pressures in 8- by 6-foot Supersonic Wind Tunnel for Mach Number Range of 0.56 to 2.07," NASA TM X-2009, May 1970.

[9]Broussinos, P. and Kabe, A. M., "Multi-Mode Random Response Analysis Procedure," USAF Space Systems Division, SSD-TR-90-53, Los Angeles, CA, Jan. 1990.

Earl A. Thornton
Associate Editor